Broad Energy Spectrum of Laser-Accelerated Protons for Spallation-Related Physics

P. McKenna,[1,*] K. W. D. Ledingham,[1,†] S. Shimizu,[1,‡] J. M. Yang,[1,§] L. Robson,[1,†] T. McCanny,[1] J. Galy,[2] J. Magill,[2] R. J. Clarke,[3] D. Neely,[3] P. A. Norreys,[3] R. P. Singhal,[4] K. Krushelnick,[5] and M. S. Wei[5]

[1]*Department of Physics, University of Strathclyde, Glasgow, G4 0NG, United Kindgom*
[2]*European Commission, Joint Research Centre, Institute for Transuranium Elements, Postfach 2340, 76125 Karlsruhe, Germany*
[3]*Central Laser Facility, Rutherford Appleton Laboratory, Chilton, Didcot, Oxon OX11 0QX, United Kingdom*
[4]*Department of Physics and Astronomy, University of Glasgow, Glasgow, G12 8QQ, United Kingdom*
[5]*Blackett Laboratory, Imperial College, London SW7 2BZ, United Kingdom*

(Received 31 August 2004; published 4 March 2005)

A beam of MeV protons, accelerated by ultraintense laser-pulse interactions with a thin target foil, is used to investigate nuclear reactions of interest for spallation physics. The laser-generated proton beam is shown (protons were measured) to have a broad energy distribution, which closely resembles the expected energy spectrum of evaporative protons (below 50 MeV) produced in GeV-proton-induced spallation reactions. The protons are used to quantify the distribution of residual radioisotopes produced in a representative spallation target (Pb), and the results are compared with calculated predictions based on spectra modeled with nuclear Monte Carlo codes. Laser-plasma particle accelerators are shown to provide data relevant to the design and development of accelerator driven systems.

DOI: 10.1103/PhysRevLett.94.084801 PACS numbers: 41.75.Jv, 25.40.Sc, 52.38.Kd

The physics of the interaction of high-intensity laser pulses with plasma to produce high energy, bright, picosecond pulsed beams of ions, neutrons, electrons, and γ radiation has generated substantial international interest recently [1]. Characterization of the accelerated particles and radiation is being used to diagnose fundamental high temperature plasma processes, including ionization and acceleration field dynamics [2–5]. This novel source of high energy particles and radiation has also been used to induce nuclear reactions, including photofission of uranium [6,7], production of radioisotopes of interest for nuclear medicine [8], and demonstration of heavy ion fusion reactions [4]. Recently, laser-plasma produced γ radiation has also been used to measure relative cross sections for transmutation reactions [9,10]. Whilst the main requirement for these experiments is satisfied by the production of a sufficiently high flux of particles or radiation above the reaction threshold energy, there are many potential applications of this unique source in the fields of nuclear and accelerator physics which would require beams of nearly monoenergetic particles, or with tailored energy distributions. In this Letter, it is shown that the characteristically broad energy distribution feature of the proton beams accelerated in laser-plasma interactions can be used to provide nuclear reaction data relevant to accelerator-based energy amplification schemes [11].

The petawatt arm of the Vulcan Nd:glass laser at the Rutherford Appleton Laboratory, UK, was used. Laser pulses with energy up to 400 J, wavelength ~ 1 μm, and average duration 0.7 ps were focused, to a peak intensity of 4×10^{20} W cm^{-2}, onto 10 μm thick, 5 mm $\times$ 5 mm, Al foil targets, at an angle of 45°. The energy distribution of accelerated protons measured at the rear of the target was diagnosed by nuclear activation of stacked Cu foils. Positron emission from ^{63}Zn, produced by (p, n) reactions on ^{63}Cu, was quantified for each copper foil using NaI-coincidence detectors, and convoluted with the well known cross sections for the ^{63}Cu$(p, n)^{63}$Zn reaction and the stopping power of protons in ^{63}Cu, to yield the proton energy spectrum shown in Fig. 1(a). This Boltzmann-like energy distribution is typical of the proton energy spectra measured in high-intensity laser interactions with thin foils [3,8].

A similarly broad energy distribution of MeV protons is produced in GeV-proton-induced spallation reactions, which are central to the development of accelerator driven systems (ADS) [12]. Proton-induced spallation reactions occur when a high energy ($\sim$GeV) proton inelastically interacts with a high-Z nucleus (typically Pb) to produce multiple secondary particles. First, the incident proton collides with a nucleus, producing secondary protons, neutrons, and pions. These secondary particles can cause further collisions in an intranuclear cascade. Second, the excited nucleus will evaporate low energy particles, or in the case of a heavy target nucleus such as Pb, the excited nucleus may fission. These processes produce a range of residual nuclei in the target. Investigation of residual nuclide production in spallation reactions is of fundamental importance to the development of ADS, to determine radiotoxicity and damage to materials. This was one of the objectives of the HINDAS project [13]. Importantly, in high energy (GeV) proton collisions with thick high-Z targets, it is the high yield of low energy (tens of MeV) secondary protons and neutrons, produced in the intranuclear cascade and through evaporation, which is largely responsible for the production of residual nuclides through secondary reactions [14].

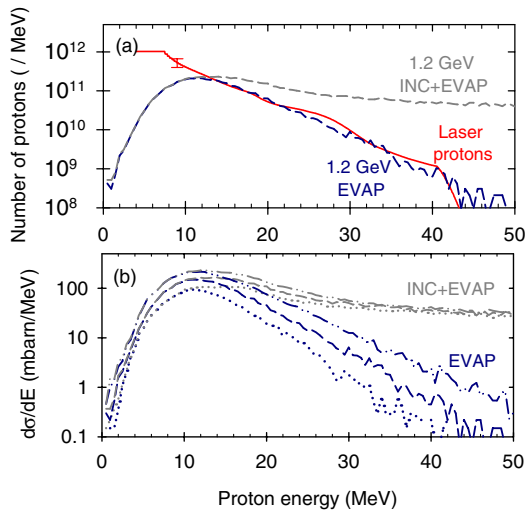

FIG. 1 (color online). (a) Proton energy spectrum (laser protons, solid line) determined via measurements of ^{63}Cu$(p, n)^{63}$Zn reactions in stacked Cu foils positioned behind a laser-irradiated 10 μm thick Al target (see text for details). (b) Calculated cross sections for proton production via spallation evaporation, EVAP, and spallation-intranuclear cascade plus evaporation, INC + EVAP, reactions in 0.8 GeV (dotted lines), 1.2 GeV (dashed lines), and 2.5 GeV (dash-dot-dotted lines) p + Pb interactions [15]. The calculated 1.2 GeV spectra (dashed lines) are shown normalized to the measured proton spectrum in (a); excellent agreement is observed with the evaporation spectrum for energies greater than 12 MeV.

Low energy proton production cross sections for 0.8, 1.2, and 2.5 GeV-proton spallation reactions on Pb, calculated using the coupled INCL2.0 (intranuclear cascade) and GEMINI (evaporation) Monte Carlo codes [15,16], are shown in Fig. 1(b). (The simulations have been carried out with the same parameters described in Enke *et al.* [16].) Herbach *et al.* [17] have found good agreement between the evaporative proton spectra predicted with these codes and experimentally measured proton spectra, for p(1.2 GeV) + W reactions. (By contrast, the codes overestimated the yield of protons below ~25 MeV produced in the intranuclear cascade.) The integrated proton yield below 45 MeV, resulting from both the intranuclear cascade and evaporation, is ~60% of all emitted protons over the full energy range (which extends up to the incident proton energy), highlighting the importance of having accurate nuclear data for residual nuclide production in this low energy regime. As shown in Fig. 1(b), although the magnitude of the cross sections increases as the incident energy increases from 0.8 to 2.5 GeV, the cross sections as a function of energy have similar shapes. The optimum incident proton energy for spallation is ~1.1 GeV, as determined by neutron multiplicity and energy consumption considerations [12,18]. For this reason the calculated spectra for the p(1.2 GeV) + Pb reaction are normalized and compared to the measured laser-generated proton spectrum in Fig. 1(a). Excellent agreement is observed with the evaporative proton energy spectrum in the important low energy region between 12 and 45 MeV. As the low energy thresholds for the dominant reactions occur at ~11 MeV (shown below), the laser-plasma-produced proton beam can be used for experimental investigation of residual nuclide production due to evaporative protons in spallation reactions.

As Pb is a representative spallation target for many ADS, residual nuclide production in a $^{\text{nat}}$Pb activation sample (1.4% ^{204}Pb; 24.1% ^{206}Pb; 22.1% ^{207}Pb; 52.4% ^{208}Pb) was investigated. A 1 mm thick, 5 cm × 5 cm sample was positioned at the rear of the laser-irradiated Al target, along the target normal direction, subtending a solid angle of 1 sr. After the laser shot, the characteristic γ rays emitted by the residual nuclei produced were measured using a calibrated germanium detector, with relative efficiency of 25% compared to the $3'' \times 3''$ NaI standard. Three spectra were measured over a total measurement time of 90 h. Characteristic γ-emission lines of product nuclides close to the target nuclei, namely ^{206}Bi, ^{205}Bi, ^{204}Bi, ^{203}Bi, ^{202}Bi, and ^{203}Pb were observed and quantified. Identification was based on the measured γ energies, intensities, and half-lives, with reference to the *Nuclides* compilation [19]. The numbers of each residual nuclide produced at the time of the laser shot (after correction for detection efficiencies, decay branching ratios, gamma emission probabilities, and half-lives) are listed, together with the relevant reaction channels and energy thresholds, in Table I.

The observed residues are mainly produced by (p, xn) reactions, which are predominant over other reactions, such as (p, f) and $(p, x\alpha)$, in the energy range 10–45 MeV. Cross sections for individual (p, xn) reactions on ^{206}Pb(x = 1–5), ^{207}Pb(x = 2–5), and ^{208}Pb(x = 3–5) were obtained from the literature [20]. Although proton-induced fission of Pb is possible, the (p, f) cross section amounts to only a small percentage of the total cross section at these energies. The cross section for ^{208}Pb(p, f), for example, is ~4 mbarn at 50 MeV, falling to 0.08 mbarn at 35 MeV [21]. No signature of proton-induced fission was observed, although the small fission cross section means that the number of fission residues produced would likely be below the detectable limit for this experiment.

The measured number of protons as a function of proton energy (Fig. 1), the proton stopping powers in Pb [22], and the experimental cross sections for the individual reactions [20] were convoluted as a function of proton energy to calculate the expected numbers of each residual nuclide produced by (p, xn) reactions. The results are listed in Table I. There is good agreement between the observed numbers and the yields calculated for the high yield residuals ^{205}Bi and ^{206}Bi. The observed numbers of ^{204}Bi and ^{203}Bi are, respectively, lower and higher by about a factor of 2 than the expected yields. These residuals are produced

via $(p, 4n)$ and/or $(p, 5n)$ reactions with cross sections in the energy range 40–50 MeV. At these energies the measured proton energy spectrum exhibits a sharp cutoff that is sensitive to laser shot-to-shot fluctuations, and this may account for the discrepancy. The observed number of ^{202}Bi is much lower than the rest of the residuals, due to the low abundance of ^{204}Pb in natural lead and the high threshold energy of the ^{206}Pb$(p, 5n)^{202}$Bi reaction (36.3 MeV). The isotope ^{207}Bi has a half-life of 38 years and is of concern for the radioactive inventory of ADS based on Pb spallation targets. Because of its long half-life, it would not have been detected in this experiment, but its production rate from ^{208}Pb$(p, 2n)$ reactions will be similar to other Bi isotopes formed by $(p, 2n)$ reactions. ^{203}Pb residuals were also observed and could be produced either by proton- or photo-induced reactions (resulting from bremsstrahlung production in the Pb sample). As the dominant reaction pathway was not unambiguously identified, no further analysis was carried out on ^{203}Pb production.

To determine how closely the measured isotopic abundances of Bi residuals compare with the expected yields, the calculated proton spectra for p(1.2 GeV) + Pb reactions (normalized to the measured proton spectrum, [Fig. 1(a)]) were also convoluted with the experimental cross sections and stopping powers. The calculated yields are listed in Table I and the ratio of each isotope yield to the total Bi yield is shown in Fig. 2. For the four main isotopes observed (^{203}Bi to ^{206}Bi) there is very good agreement between the isotopic distributions calculated using the measured proton spectrum and the calculated spectrum of evaporative protons. As discussed above, the experimental measurements of the isotopic distributions are also in good agreement, especially for the high yield isotopes ^{205}Bi and ^{206}Bi. The expected isotopic distribution is substantially different, however, when protons from the intranuclear cascade are included. This is due to the increased flux of protons in the energy range between 30 and 50 MeV (Fig. 1), which enhances contributions to $(p, 3n)$ reactions leading to ^{205}Bi and ^{206}Bi, and substantially increases the yield of ^{202}Bi, ^{203}Bi, and ^{204}Bi, produced by $(p, 4n)$ and/or $(p, 5n)$ reactions with cross sections peaked at high energies. The expected overall effect is a change in the isotopic distribution in favor of the lighter Bi isotopes, as shown in Fig. 2.

In summary, a laser-generated beam of protons has been used to investigate residual nuclide production due to protons evaporated in GeV spallation reactions on Pb. In general, the production of residues in spallation targets is

TABLE I. Residual nuclei produced in the ^{nat}Pb activation sample positioned at the rear of the laser-irradiated Al foil target. Proton-induced reactions and threshold energies, E_{Thresh}, are listed. The observed numbers of each nucleus, per laser shot, have been determined after correction for detection efficiencies, decay branching ratios, gamma emission probabilities, and half-lives (listed). The calculated numbers of each nucleus have been determined by convoluting proton energy spectra with the experimental cross sections [20]. Results labeled $\sum$ correspond to a summation over the contributions from the individual reaction channels. The calculation was carried out using the measured laser-plasma-accelerated proton energy spectrum and the calculated p(1.2 GeV) + Pb evaporation (EVAP) and intranuclear cascade plus evaporation (INC + EVAP) spectra [15].

Observed residuals	Half-life	Observed no. of residual nuclei	Reactions	E_{Thresh} (MeV)	Calculated expected no. of residual nuclei		
					Laser protons	EVAP	INC + EVAP
^{202}Bi	1.67 h	$(1.2 \pm 0.8) \times 10^6$	^{204}Pb$(p, 3n)^{202}$Bi	21.4	...	...	...
			^{206}Pb$(p, 5n)^{202}$Bi	36.3	8.2×10^4	7.0×10^5	1.3×10^8
^{203}Bi	11.76 h	$(2.3 \pm 0.3) \times 10^7$	^{204}Pb$(p, 2n)^{203}$Bi	12.5	...	...	...
			^{206}Pb$(p, 4n)^{203}$Bi	27.4	8.7×10^6	8.7×10^6	5.1×10^8
			^{207}Pb$(p, 5n)^{203}$Bi	34.2	8.2×10^4	7.0×10^5	1.2×10^8
					$\sum 8.8 \times 10^6$	$\sum 9.4 \times 10^6$	$\sum 6.3 \times 10^8$
^{204}Bi	11.22 h	$(6.4 \pm 0.9) \times 10^7$	^{204}Pb$(p, n)^{204}$Bi	5.3	...	...	...
			^{206}Pb$(p, 3n)^{204}$Bi	20.2	1.1×10^8	8.5×10^7	7.0×10^8
			^{207}Pb$(p, 4n)^{204}$Bi	26.9	5.5×10^6	5.0×10^6	3.4×10^8
			^{208}Pb$(p, 5n)^{204}$Bi	34.3	...	...	...
					$\sum 1.2 \times 10^8$	$\sum 9.0 \times 10^7$	$\sum 1.0 \times 10^9$
^{205}Bi	15.31 d	$(5.9 + 0.9) \times 10^8$	^{206}Pb$(p, 2n)^{205}$Bi	11.6	3.9×10^8	3.8×10^8	1.2×10^9
			^{207}Pb$(p, 3n)^{205}$Bi	18.4	9.0×10^7	6.7×10^7	5.4×10^8
			^{208}Pb$(p, 4n)^{205}$Bi	25.8	1.7×10^7	1.6×10^7	9.0×10^8
					$\sum 5.0 \times 10^8$	$\sum 4.7 \times 10^8$	$\sum 2.7 \times 10^9$
^{206}Bi	6.24 d	$(5.8 \pm 0.9) \times 10^8$	^{206}Pb$(p, n)^{206}$Bi	4.6	...	...	...
			^{207}Pb$(p, 2n)^{206}$Bi	11.3	2.9×10^8	2.9×10^8	7.1×10^8
			^{208}Pb$(p, 3n)^{206}$Bi	18.7	2.5×10^8	1.9×10^8	1.6×10^9
					$\sum 5.4 \times 10^8$	$\sum 4.8 \times 10^8$	$\sum 2.3 \times 10^9$

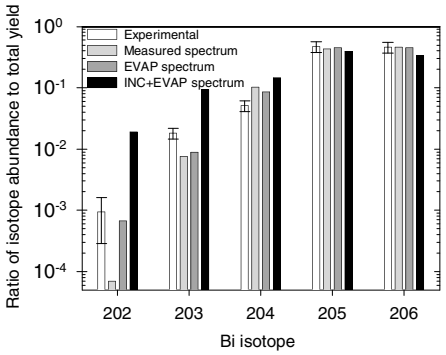

FIG. 2. Isotopic distributions of Bi residues in ^{nat}Pb produced by protons with energy up to 50 MeV. The ratios of the yield of each isotope to the total Bi yield, as measured experimentally (white) and calculated (gray/black) using the experimental cross sections [20] and the experimental and theoretical proton spectra, are plotted.

complicated by the range of primary and secondary particles produced in competing spallation processes, and therefore codes are widely relied upon to calculate nuclide production due to specific processes [14]. Low energy ($<$45 MeV) secondary protons produced both in the intranuclear cascade and by evaporation contribute significantly to residual nuclide production. This work illustrates that high power laser-based accelerators, producing proton beams with broad energy distributions, can be used to experimentally determine residual nuclide generation arising from specific spallation processes, namely, evaporation. Potentially useful experimental data for the development of codes simulating nuclide production in spallation targets are obtained.

Projected developments in laser-particle accelerators will enable these novel particle sources to be used for similar studies of other spallation processes in the future. Recent particle-in-cell simulations suggest that by carefully controlling the laser-irradiated target parameters it should be possible to tailor the shape of the energy spectrum of accelerated protons [23]. This would enable measurement of residue production due to protons produced in the intranuclear cascade and other spallation reactions. Furthermore, as focused laser intensities increase to between 10^{22} and 10^{23} W cm^{-2}, protons with upper energies in the range 250 MeV to 1 GeV are expected to be produced, facilitating laser-driven investigations of proton-induced fission and other intermediate and high energy spallation processes.

We acknowledge the expert assistance of the Vulcan operations teams. We gratefully acknowledge D. Hilscher and C.-M. Herbach for providing us with the calculated proton spectra for p + Pb spallation reactions. P. M. acknowledges support from the Royal Society of Edinburgh. S. S. and J. M. Y. acknowledge support from the Japan Society for the Promotion of Science and the China Scholarship Council, respectively.

*Electronic mail: p.mckenna@phys.strath.ac.uk
†Also at A.W.E., Aldermaston, Reading RG7 4PR, United Kingdom.
‡Present address: Institute for Chemical Research, Kyoto University, Gokasho, Uji, Kyoto 611-0011, Japan.
§Present address: Research Center of Laser Fusion, P.O.Box 919-986, Mianyang, 621900, People's Republic of China.

[1] K. W. D. Ledingham, P. McKenna, and R. P. Singhal, Science **300**, 1107 (2003).
[2] E. L. Clark *et al.*, Phys. Rev. Lett. **85**, 1654 (2000).
[3] M. Hegelich *et al.*, Phys. Rev. Lett. **89**, 085002 (2002).
[4] P. McKenna *et al.*, Phys. Rev. Lett. **91**, 075006 (2003).
[5] M. Borghesi *et al.*, Phys. Rev. Lett. **88**, 135002 (2002).
[6] K. W. D. Ledingham *et al.*, Phys. Rev. Lett. **84**, 899 (2000).
[7] T. E. Cowan *et al.*, Phys. Rev. Lett. **84**, 903 (2000).
[8] K. W. D. Ledingham *et al.*, J. Phys. D **37**, 2341 (2004).
[9] K. W. D. Ledingham *et al.*, J. Phys. D **36**, L79 (2003).
[10] J. Magill *et al.*, Appl. Phys. B **77**, 387 (2003).
[11] C. Rubbia *et al.*, CERN Internal Report No. CERN-AT-95-44 ET, 1995 (unpublished).
[12] N. Watanabe, Rep. Prog. Phys. **66**, 339 (2003).
[13] See the HINDAS project homepage at http://www.fynu.ucl.ac.be/collaborations/hindas/.
[14] M. Gloris *et al.*, Nucl. Instrum. Methods Phys. Res., Sect. A **463**, 593 (2001).
[15] D. Hilscher and C.-M. Herbach (private communication).
[16] M. Enke *et al.*, Nucl. Phys. **A657**, 317 (1999).
[17] C.-M. Herbach *et al.*, *Proceedings of the International Workshop on Nuclear Data for the Transmutation of Nuclear Waste*, edited by Aleksandra Kelic and Karl-Heinz Schmidt (GSI, Darmstadt, 2003).
[18] D. Hilscher *et al.*, J. Nucl. Mater. **296**, 83 (2001).
[19] J. Magill, *Nuclides.net: An Integrated Environment for Computations on Radionuclides and Their Radiation* (Springer-Verlag, Berlin, 2003).
[20] R. E. Bell and H. M. Skarsgard, Can. J. Phys. **34**, 745 (1956).
[21] A. V. Prokofiev, Nucl. Instrum. Methods Phys. Res., Sect. A **463**, 557 (2001).
[22] J. F. Ziegler, J. P. Biersack, and U. Littmark, *The Stopping and Ranges of Ions in Solids* (Pergamon Press, New York, 1985).
[23] T. Z. Esirkepov *et al.*, Phys. Rev. Lett. **89**, 175003 (2002).